

Critical rf Magnetic Fields for Some Type-I and Type-II Superconductors

T. Yogi, G. J. Dick, and J. E. Mercereau

Department of Physics, California Institute of Technology, Pasadena, California 91125

(Received 23 May 1977)

The critical rf magnetic field H_c^{rf} of several type-I and type-II superconductors has been measured between 90 and 300 MHz and near T_c has been found to approach the ideal superheating field in nearly all cases. However, in the same samples the dc critical field shows little evidence of superheating. The temperature dependence of H_c^{rf} suggests that rf-stimulated vortex nucleation occurs in the type-I materials.

The critical rf magnetic field H_c^{rf} of several type-I and type-II superconductors ($0.06 < \kappa < 1.8$) has been measured at frequencies ranging from 90 to 300 MHz. Near the transition temperature T_c for both type-I and -II superconductors, the measured critical field H_c^{rf} for ~ 1 -mm-diam spherical samples is consistent in magnitude with the calculated zero-frequency (or dc) superheating field¹ H_{sh} for these materials. The calculations of H_{sh} were based on an experimental evaluation² of the Ginzburg-Landau parameter κ , transition temperature T_c , thermodynamic critical field H_c , etc., for the samples. However, the dc critical magnetic field was also measured and little ($\approx 10\%$) dc superheating was observed, presumably because of surface defects in these relatively large samples. Previous dc measurements³ for some of these materials, in aggregates of small ($\sim 10 \mu\text{m}$) spheres, do show the ideal calculated superheating effects.³ From the temperature dependence of H_c^{rf} in type-I materials, it can be inferred that the rf-induced phase transition to the normal state is by vortex nucleation.

These experiments were done with use of the elemental superconductors In, Sn, and Pb, and a series of alloys of SnIn and InBi. The large rf magnetic fields were developed in a helically loaded superconducting Nb resonator driven by a phase-locked, voltage-controlled oscillator. The resonator was usually operated in a pulsed mode to minimize sample heating and H_c^{rf} was defined to be the field amplitude at which the resonator Q was degraded due to dissipation in the sample. At field amplitude below H_c^{rf} the sample was always completely superconducting and thermally stable. Measurements in high rf magnetic fields were done at ambient dc-field levels $< 10^{-2}$ G. Data for H_c^{rf} were found to be independent of the dc field up to about 10^{-1} G where flux trapping begins to cause serious degradation. Spherical samples were prepared from commercially obtained, 99.999%-purity materials, by cooling a

droplet of the melt in free fall and then annealed as necessary to assure homogeneity. The samples were thermally grounded by a sapphire rod and located at a position of maximum rf field; H_c^{rf} was indicated by an abrupt decrease in resonator Q as the rf-field amplitude at the sample surface was increased above H_c^{rf} . Fields in the resonator were carefully calibrated and cross-checked in several ways. The electronic calibration techniques themselves were finally evaluated by using a resonator as a particle accelerator and comparing the calibrated fields within the resonator against the measured energy gain by the particles.

For all samples the zero-frequency thermodynamic critical fields H_c and/or H_{c1} were experimentally determined by measuring the low-frequency (100–1000 Hz) susceptibility as a function of static applied field H . From the variation of susceptibility with H , a determination of H_c , H_{c1} , H_{c2} , H_{c3} , the dc superheating and supercooling fields, etc., could be determined by standard techniques.³ Experimental values of H_c and T_c for the elemental superconductors were obtained from several samples and all agreed with the accepted standard values to within a few percent. This correspondence thus supports the reliability of the calibration techniques and the assumptions regarding important experimental parameters such as demagnetizing factors, etc. However, in these low-frequency susceptibility measurements superheating effects were found to be limited in general to $< 10\%$ and in no case did the dc superheating field approach the magnitude of H_c^{rf} .

Data for the reduced field $h_c^{rf} = H_c^{rf}/H_c$ versus reduced temperature $t = T/T_c$ are shown in Fig. 1 for a typical Sn sphere. For these samples, the maximum dc superheating fields were also measured but were found to be limited to $\leq 1.1H_c$. Figure 1 also indicates the the temperature dependences to be expected for the ideal dc superheating field based on different assumptions regarding the geometry of flux entry into the super-

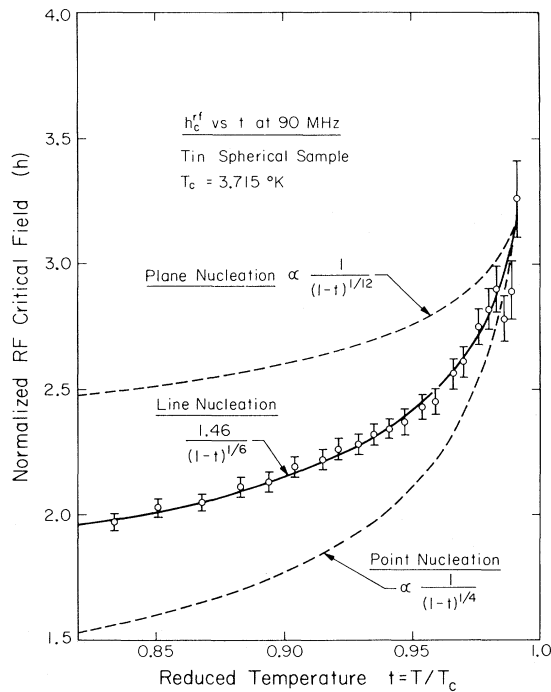


FIG. 1. Data points represent the normalized rf critical field $h_c^{rf} = H_c^{rf}/H_c$ for Sn at 90 MHz vs reduced temperature $t = T/T_c$. Curves represent theoretical estimates of dc superheating for several phase-boundary configurations. Previous dc measurements (Ref. 3) near T_c range from about 2.8–3.1.

conductor. Basically, the superheating field is determined by balancing the loss in condensation energy against the gain in diamagnetic energy which accompanies the formation of a phase boundary in a field H . Most calculations have been done in a one-dimensional limit for which this balance occurs at a plane boundary when the energies per unit area are equal or, when $\lambda H^2 \approx \xi H_c^2$. Thus, the normalized dc superheating field $h_p = H_{sh}/H_c \propto (\xi/\lambda)^{1/2} = (\mathcal{K})^{-1/2}$, where ξ and λ are, respectively, the coherence length and penetration depth. Both ξ and λ are temperature-dependent quantities. In the nonlocal limit appropriate to pure Sn and In detailed calculations³ for a plane boundary have shown that the temperature dependence of h_p is given by $h_p \approx 1.04\mathcal{K}_0^{-1/3}(1-t)^{-1/12}$. For Sn, $\mathcal{K}_0 \approx 0.09$ and the calculation predicts $h_p \approx 2.2(1-t)^{-1/12}$. This expression is plotted in Fig. 1, as the dashed line labeled plane nucleation. Thus, near T_c the magnitude of the experimental h_c^{rf} is consistent with the analytic prediction for h_p . However, at lower temperatures the temperature dependence of h_c^{rf} is more rapid than that expected for planar nucleation or

observed in previous dc measurements.³

The other curves shown in Fig. 1 result from applying the basic energy-balance relationship to the creation of a vortex and to point nucleation. For vortex nucleation, equating energy per unit length gives $\lambda^2 H^2 \approx \xi^2 H_c^2$ or $h_v \propto \mathcal{K}^{-1}$, while point nucleation requires $h_i \propto \mathcal{K}^{-3/2}$. Evaluating \mathcal{K} in the nonlocal limit leads to $h_v \propto \mathcal{K}_0^{-2/3}(1-t)^{-1/6}$ and $h_i \propto \mathcal{K}_0^{-1}(1-t)^{-1/4}$ for these cases. These temperature dependences are shown in Fig. 1 normalized to $t = 0.99$. The data are consistent with a vortex-nucleation model and lead to an evaluation of the proportionality constant for h_v in the nonlocal limit as $h_v = 0.33\mathcal{K}_0^{-2/3}(1-t)^{-1/6}$.

Similar results relating h_c^{rf} and h_v were also found for In with the same proportionality constant. Extensive data have not yet been taken for Pb, however significant superheating also persists at lower temperatures. For example, for Pb, $h_c^{rf} = 1.4$ at $t = 0.3$. The implication of these results is that surface defects play a lesser role in nucleating the rf magnetic transition than they do in nucleating the dc transition. Nevertheless, except very close to T_c , the rf transition occurs at a lower field intensity than the ideal value H_{sh} and has a temperature dependence corresponding to vortex nucleation even in type-I materials.

Alloy samples of SnIn (0–6.3 at.% In) were prepared in a range of the Ginzburg-Landau parameter \mathcal{K} ($0.09 < \mathcal{K} < 1.0$) and alloys of InBi (0–4 at.% Bi) in the range ($0.16 < \mathcal{K} < 1.8$). The droplet samples were subsequently annealed after formation for many hours near their melting temperature. Similar alloy samples were consistent in their superconducting properties to within experimental accuracy and in general the width in T_c for a given alloy sample was $\sim 10^{-2}$ °K. Values of \mathcal{K} for the alloys were determined by using the Gor'kov-Goodman equation⁴ and measured values of the resistivity for the samples. Sample resistance was determined by both a dc four-terminal technique and from measurements of rf surface resistance from changes in resonator Q . These two techniques agreed to within 5%. The results for \mathcal{K} , T_c , and H_c as a function of In or Bi concentration were in very good agreement with previous results on these alloys.^{3,5} For example, in the InBi system as Bi ranged from 0 to 4 at.%, \mathcal{K} varied from 0.06 to 1.75, T_c varied from 3.40 to 4.41°K, and H_c^0 varied from 280 to 510 G. Measurements of H_c^{rf} and H_c for the alloy samples were done by the techniques previously described for the pure materials.

For the alloy samples, the temperature depen-

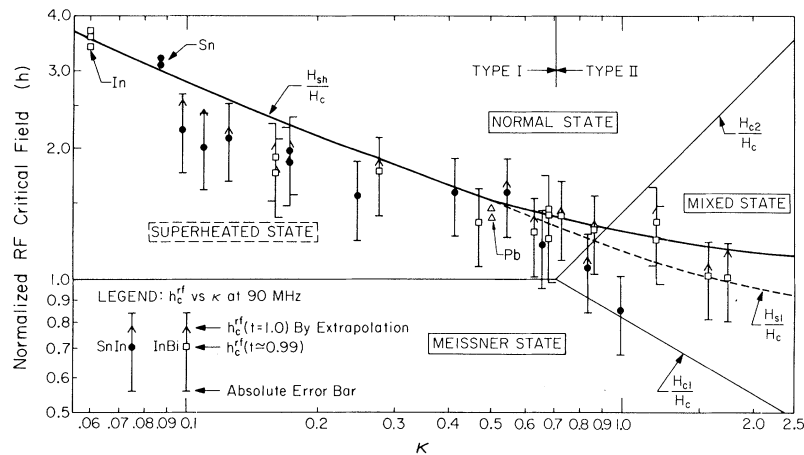


FIG. 2. Normalized critical field as a function of the Ginsburg-Landau parameter κ . Data points are for h_c^{rf} at $t=0.99$ for several metals and alloys. Full curve is calculation (Matricon and St. James, Ref. 1) of the dc superheating field h_p ; dashed curve is the fluctuation-limited field estimated by Kramer (Ref. 1).

dence of h_c^{rf} was in general found to be much less pronounced than for the pure materials illustrated in Fig. 1. This tendency is anticipated by the local-limit theories which should apply to these short-mean-free-path samples. In the local limit $h_v \propto (1+t^2)$ while $h_p \propto (1+t^2)^{1/2}$. Thus in this limit, h varies relatively slowly near T_c . These temperature dependences do represent the trend in the alloy data for h_c^{rf} to increase near T_c , but there was no clear experimental basis to choose between them. In fact, it was not possible to find a universal temperature functional dependence to fit all alloys. Consequently, a relative evaluation of h_c^{rf} near T_c is shown in Fig. 2 as a function of κ .

Figure 2 shows experimental values for h_c^{rf} near T_c at 90 MHz plotted as a function of κ for several alloys of SnIn and InBi, as well as for In, Sn, and Pb. Data points are predominately given for $t=0.99$ but where possible extrapolation of the data to $t=1$ by analytic continuation is included as an arrow. Also shown in Fig. 2 are calculations of h_p in the local limit at T_c as a function of κ . The full line follows a calculation by Matricon and St. James¹ while the dashed line follows Kramer.¹ Measurements of h_c^{rf} were made also at frequencies up to 300 MHz for several samples ($0.06 < \kappa < 1.5$), however, no significant difference from 90-MHz results were found in the magnitude or temperature dependence of superheating.

These alloy data span from type-I to type-II materials ($0.06 < \kappa < 1.8$). Also included are a few examples of data from different spherical samples at the same κ to indicate the degree of

internal consistency. In the type-I region, $\kappa < \sqrt{2}^{-1}$, the alloy data for h_c^{rf} indicate a consistent tendency to approach the dc superheating field h_p as $T \rightarrow T_c$. In the type-II region, the tendency for h_c^{rf} to approach the theoretical superheating limit persists for alloys of InBi. However, for SnIn, the trend is toward the lower thermodynamic critical field, H_{c1} . Contrary to what might have been expected, microscopic examination of the spherical surfaces indicated SnIn to be considerably smoother than InBi. Thus surface condition alone will not explain the above divergent behavior.

These experiments indicate that rf superheating is less sensitive to surface defects than dc superheating for both type-I and -II superconductors. For the type-I materials Sn, In, and Pb, the amplitude of h_c^{rf} , near T_c , was found to be consistent with the dc planar superheating field h_p . However, the temperature dependence of h_c^{rf} may indicate that vortex nucleation dominates at lower temperatures, causing h_c^{rf} to fall below h_p . For type-I alloys it was also found that h_c^{rf} approached h_p near T_c , while for type-II alloys h_c^{rf} ranged from h_p to h_{c1} depending on the particular composition. These results are consistent with the previously noted trend⁶ in some type-II materials to exclude flux at fields considerably in excess of H_{c1} . The results also suggest that, if the vortex is created within one rf cycle, the time scale for vortex nucleation in these experiments as less than 10^{-9} sec.

This work was supported by National Science Foundation Grants No. PHY76-20406 and PHY76-

81713.

¹V. L. Ginzburg, *Zh. Eksp. Teor. Fiz.* **34**, 113 (1958) [*Sov. Phys. JETP* **7**, 78 (1958)]; J. Matricon and D. St. James, *Phys. Lett.* **24A**, 241 (1967); H. J. Finkand and A. G. Presson, *Phys. Rev.* **182**, 498 (1969); L. Kramer, *Phys. Rev.* **170**, 475 (1968), and *Z. Phys.* **259**, 333 (1973); H. Parr, *Phys. Rev. B* **12**, 4886 (1975), and **14**, 2842, 2899 (1976).

²T. Yogi, thesis, California Institute of Technology, 1976 (unpublished).

³F. W. Smith, A. Baratoff, and M. Cardona, *Phys.*

Kondens. Mater. **12**, 145 (1970).

⁴L. P. Gor'kov, *Zh. Eksp. Teor. Fiz.* **37**, 1407 (1959) [*Sov. Phys. JETP* **10**, 998 (1960)]; B. B. Goodman, *IBM J.* **6**, 63 (1962).

⁵T. Kinsel, E. A. Lynton, and B. Serin, *Rev. Mod. Phys.* **36**, 105 (1964); I. Kirschner *et al.*, *Zh. Eksp. Teor. Fiz.* **66**, 2141 (1974) [*Sov. Phys. JETP* **39**, 1054 (1974)].

⁶R. Shaw, B. Rosenblum, and F. Bridges, *IEEE Trans. Magn.* **13**, 811 (1976); P. Kinsel *et al.*, *IEEE Trans. Magn.* **13**, 496 (1976); B. Hillenbrand *et al.*, *IEEE Trans. Magn.* **13**, 491 (1976); D. F. Moore and M. R. Beasley, *Appl. Phys. Lett.* **30**, 494 (1977).

Proper Ferroelastic Transition in Piezoelectric Lithium Ammonium Tartrate

Akikatsu Sawada

*Synthetic Crystal Research Laboratory, Faculty of Engineering, Nagoya University,
Chigusa-ku, Nagoya 464, Japan*

and

Masayuki Udagawa

Department of Physics, Waseda University, Shinjuku-ku, Tokyo 160, Japan

and

Terutaro Nakamura

Institute for Solid State Physics, The University of Tokyo, Roppongi Minato-ku, Tokyo 106, Japan

(Received 13 June 1977)

Dielectric and Brillouin scattering experiments on a lithium ammonium tartrate crystal have shown that the transition in this crystal is described by the free energy of a piezoelectric crystal,

$$F = \frac{1}{2}(\chi^x)^{-1}P^2 + aPx + \frac{1}{2}\beta(T - T_0)x^2,$$

where the primary order parameter is the homogeneous strain, which gives rise to ferroelectricity through the piezoelectric coupling with the polarization.

At present, ferroelasticity is a well-accepted concept. However, many ferroelastic crystals so far reported do not undergo the "proper ferroelastic" transition in which the primary order parameter is the homogeneous strain x . Here, we treat the ferroelastic transition, which is described by the free energy with a bilinear coupling term,

$$F = \frac{1}{2}(\chi^x)^{-1}P^2 + aPx + \frac{1}{2}C^P x^2, \quad (1)$$

and we conclude that the transition of $\text{LiNH}_4\text{C}_4\text{H}_4\text{O}_6 \cdot \text{H}_2\text{O}$ (LAT) at 98 K is a "proper ferroelastic" transition.

In KH_2PO_4 , the transition is well described by the free energy

$$F_1 = \frac{1}{2}\alpha(T - T_0)P^2 + aPx + \frac{1}{2}C^P x^2, \quad (2)$$

where the piezoelectric coefficient a and the elas-

tic stiffness at constant polarization, C^P , are independent of temperature. In the early stages of the investigation of $\text{Gd}_2(\text{MoO}_4)_3$, the transition was suggested to be described by the free energy

$$F_2 = \frac{1}{2}(\chi^x)^{-1}P^2 + aPx + \frac{1}{2}\beta(T - T_0)x^2, \quad (3)$$

where a and the clamped inverse susceptibility $(\chi^x)^{-1}$ are independent of temperature. $\text{Gd}_2(\text{MoO}_4)_3$ was, however, shown to undergo the transition because of the softening of zone-boundary phonons,¹ and is not described by Eq. (3).

The present work reports the observation of the ferroelastic transition, described by the free energy F_2 [Eq. (3)], in the crystal $\text{LiNH}_4\text{C}_4\text{H}_4\text{O}_6 \cdot \text{H}_2\text{O}$. LAT undergoes the transition at $T_c = 98$ K, the ferroelectric phase below T_c belongs to $P12_11$, and the paraelectric phase above T_c belongs to $P2_12_12$. According to the ESR study of Cr^{3+} in